Journal of Ceramic Processing Research. Vol. 23, No. 3, pp. 304~311 (2022)
(Received 22 November 2021, Received in revised form 21 January 2022, Accepted 25 January 2022)
https://doi.org/10.36410/jcpr.2022.23.3.304

J O U R N A L O F
Ceramic Processing Research

TiO_2 addition into nuclear glass ceramic: Study of the crystalline phases, structure and chemical durability

Rafika Souag[a,*], Nour elhayet Kamel[b], Dalila Moudir[b], Yasmina Mouheb[b] and Fayrouz Aouchiche[b]
[a]*Research Unit, Materials, Processes and Environment (URMPE), University of Boumerdes, Algeria*
[b]*Environment, Safety and Radioactive Waste Division , Nuclear Research Centre of Algiers, 2. Bd frantz Fanon, BP : 399, Alger-RP9, Algiers, Algeria*

This paper studies the nuclear glass ceramic based on aluminosilicate glass. It is proposed the addition of TiO_2 on the crystalline phase. The structure and chemical durability have been investigated. The materials with four TiO_2 contents, ranging from 4.11 to 7.11 wt.%, are synthesized by a discontinuous method. The 7.11 wt.% TiO_2 glass ceramic synthesis was not successful and crystallizes during the melting stage. For the others materials, Archimedes density ranges between 2.891 and 2.962 g/cm^3. For the majority of materials, X-ray diffraction analysis allows the identification of an aluminosilicate that belongs to pyroxenes silicates family as the initial phase, powelite and calzirtite. These phases are known as radionuclides' sequestration minerals. Both SEM and DTA analyses confirm these findings. The FTIR analysis of materials reveals the complex glass-ceramics chemical composition. MCC1 and MCC2 tests, performed on selected glass ceramic materials, indicate that the materials containing 4.11 and 5.11 wt.% TiO_2 are the most durable against Si, Al, Mg and Ce elements release, in MCC2 test; the Ce (minor actinide surrogate) leaching rate being negligible (193.7×10^{-9} kg/m^{2}d after 28 leaching days for 5.11 wt.% of TiO_2 content). These results make valuable conclusions for the selection of the glass ceramic suitable to the high-level waste disposal.

Keywords: Nuclear glass ceramics, TiO_2, Pyroxenes, XRD, Chemical durability.

Introduction

The radioactive waste (RW) storage and disposal is a difficult task. It requires meticulous control. One of the RW disposal principles is to follow the waste through all stages of its life: packaging, storage, disposal, and monitoring until its radioactivity is comparable to natural background radiation [1]. Several sequestration materials have been studied, among glasses, minerals, and glass-ceramic matrices.

Specifically, for the glass ceramic matrices, the sequestration occurs for the whole radionucleides present in a liquid waste solution [2, 3].

Nevertheless, because of both their high chemical durability and high ability to incorporate specific radionuclides, several ceramic matrices such as zirconates, titanates and phosphates have been proposed. This permits the long-lived radionuclides immobilization such as minor actinides [4-6].

The ceramics elaboration processes are hard to apply, and many glass-ceramics are also under study. They are constituted of crystals distributed in a glass matrix with a performance improvement. Research on glass-ceramics (noted: GC) matrices for RW sequestration will be aided by both glass technology and the intriguing crystalline ceramic phases confinement features. Different nucleating agents added to a chosen parent glass present a significant impact on the crystallization processes and the physico-mechanical properties of a given GC [7, 8]. The nucleating agents effect such as ZrO_2 and TiO_2 on the crystallization, microstructure and durability properties of the prepared GC are described in the literature [9-11].

Despite the TiO_2's significance role in the silicate glasses structure. Till now, only a few researches have been carried out [12]. In silicate melts, TiO_2 is proven to be quite soluble.. It decreases the melt glass viscosity [7]. TiO_2 addition influences the crystalline phase nature and the microstructure formed in the GC materials in addition to their physico-mechanical properties [13, 14]. Zhou et al. [15] noted that TiO_2 is often used to facilitate nucleation in silicate glass-ceramics systems. The TiO_2 content effect on the crystalline phases, structure, and aqueous dissolution rate of iron phosphate based glass ceramic waste was deeply studied by Fu Wang et al. [16].

In this work, we have synthesized a TiO_2-rich GC by a discontinuous method, consisting in a double melting at 1350 °C, followed by both a crystallization and crystal-growth, treatments at 564 °C and 1010 °C, respectively. In order to study this addition effect on the

*Corresponding author:
Tel : +00 213 661 751 789
Fax: +00213 24 79 9423
E-mail: r.souag@univ-boumerdes.dz

crystalline phases, structure and chemical durability for the nuclear GC, constituted by an aluminosilicate glass in the system: SiO_2-Al_2O_3-CaO-MgO-ZrO_2-TiO_2. Four TiO_2 compositions, ranging from 4.11 wt% to 7.11 wt% are synthetized. Then, the materials densities are measured. Different characterisations are performed such: (X-ray Diffraction (XRD), Scanning Electronic Microscopy (SEM), Differential Thermal Analysis (DTA) and Fourier Transform Infrared Spectroscopy (FTIR)). Finally, chemical durability testing was carried out using the standard MCC-1 and MCC-2 static leach test methods at 25 °C and 90 °C, respectively.

Experimental

The GC chemical compositions are inspired from the previous research studies [17, 18]. The samples are prepared with the following TiO_2 contents: 4.11 wt.%, 5.11 wt.%, 6.11 and 7.11 wt.% (Table 1). The corresponding glass ceramics are noted: GC1, GC2, GC3, GC4, respectively.

The employed commercial reagents are: Al_2O_3 (Fluka), B_2O_3 (Purity ≥99%), CaO (Merck, ≥97%), CeO_2 (Aldrich, 99.999%), CrO_3 (Merck, ≥99%), Fe_2O_3 (Merck, ≥99%), K_2CO_3 (Merck, ≥99%), Li_2O (Merck, ≥99%), MgO (Flucka, ≥97%), MnO_2 (Merck), MoO_3 (Merck, ≥99.5%), Nd_2O_3 (Fluka, ≥99.9%), P_2O_5 (Merck, ≥98%), Pr_6O_{11} (Merck, ≥99%), SiO_2 (Prolabo), Ta_2O_5 (Merck, ≥99%), TiO_2 (Merck, ≥99%),V_2O_5 (Labosi), WO_3 (Merck), Y_2O_3 (Merck, ≥99%), Yb_2O_3 (Aldrich, 99.9%), ZrO_2 (Aldrich, 99%). REE elements' oxides are dried over night at 1000 °C, and the other oxides at 400 °C, for the same time. BaO, Er_2O_3, La_2O_3 and NiO are prepared by calcination at 450 °C of $BaNO_3$ (Fluka, 99.6%), $ErN_3O_9{\cdot}5H_2O$ (Acros Organics, 99.9%), $La(NO_3)_3{\cdot}6H_2O$ (Fluka, 99.99%), and $Ni(NO_3)_2{\cdot}6H_2O$ (Fluka, 99.6%), respectively.

The GC synthesis is obtained by a double melting at 1350 °C. This is necessary to ensure the complete oxides mixture homogenization and thus isotropic properties of the final products. The melts are poured in a graphite cylindrical mold to get pellets. The nucleation step is carried out at temperature Tn during 2 h, such that: Tn = Tg + 30 °C, with Tg is the glass transition temperature. The crystal growth treatment (Tc) is performed at 1010 °C for 3 h, for the whole materials. They are finally cooled to ambient air. Both Tg and Tc are deducted from the DTA (differential thermal analysis) parent glass diagram. The detailed DTA diagrams are given in the previous study [17].

The materials Archimedes density is measured by pycnometer with water as a wetting liquid. The XRD analysis is performed out using a PANALytical X'Pert Pro diffractometer equipped with the copper anticathode, Kα1 = 1.5418Å. The analys is done with 40 kV voltage of and 40 mA current intensity. For 2θ ranging between 3 and 80°. The ceramics phase identification is performed using a Philips X'Pert High Score Plus software, version 4.1 [19]. While the materials microstructure is revealed by SEM microscopy observations, conducted by Philips XL30 microscope.

Table 1. Chemical composition of the synthesized GC materials

Oxides (wt.%)	Content (%)			
	GC1	GC2	GC3	GC4
TiO_2	4.110	5.110	6.110	7.110
Al_2O_3	13.040	13.040	13.040	13.040
B_2O_2	0.800	0.800	0.800	0.800
BaO	1.600	1.600	1.600	1.600
CaO	9.000	9.000	9.000	9.000
CeO_2	3.010	3.010	3.010	3.010
CrO_3	0.400	0.400	0.400	0.400
Er_2O_3	1.310	1.310	1.310	1.310
Fe_2O_3	1.310	1.310	1.310	1.310
K_2O	0.670	0.670	0.670	0.670
La_2O_3	0.500	0.500	0.500	0.500
Li_2O	4.220	4.220	4.220	4.220
MgO	3.500	3.500	3.500	3.500
MnO_2	0.200	0.200	0.200	0.200
MoO_3	2.810	2.810	2.810	2.810
Nd_2O_3	1.200	1.200	1.200	1.200
NiO	0.600	0.600	0.600	0.600
P_2O_5	0.400	0.400	0.400	0.400
Pr_6O_{11}	0.100	0.100	0.100	0.100
SiO_2	49.02	48.020	47.02	46.02
Ta_2O_5	0.200	0.200	0.200	0.200
V_2O_5	0.100	0.100	0.100	0.100
WO_3	0.800	0.800	0.800	0.800
Y_2O_3	0.500	0.500	0.500	0.500
Yb_2O_3	0.100	0.100	0.100	0.100
ZrO_2	0.500	0.500	0.500	0.500
Total	100.000	100.000	100.000	100.000

The GCs DTA analysis with different TiO_2 contents is performed using NETZSCH STA 409 PC device on powders, for which 11 to 25 mg in alumina crucible powder, is heated into (20% N_2-80% O_2) atmosphere at 15 °C/min up to 1050 °C.The analyzes are carried out in the temperature range from 20 to 1450 °C.

The FTIR spectra are recorded from 4000 to 400 cm^{-1} (wave numbers) by a standard KBr pellet method using a NICOLET 380 spectrometer. The pellets are prepared by mixing glass powder about (1-2 mg) with anhydrous KBr (100-200 mg). The resolution of the device is 4 cm^{-1}. The spectra data processing is performed by the OMNIC software [20].

Two IAEA standard static leaching tests, MCC1 and MCC2, are used out on GC materials that are selected from different TiO_2 contents [21]. The Surface/Volume ratio must be constant throughout the test and equal to 1/10. The GC materials cylindrical pellets are immersed in bi-distilled water, in dark glass bottles. MCC1 leach test is performed at ambient temperature (25±1) °C in

opened bottles, and MCC2 leach test in closed bottles, left in an oven heated at (90±1) °C. For both tests, water samplings are performed at: 1, 3, 7, 14, 21, 36, 42 and 96 days. The kinetic dissolution materials was performed following: Si, Al, Mg and Ce (actinide surrogate), elements dissolution in the leachates. The dissolution speed is assessed by PANALytical Magi-xPro wavelength dispersive X-ray fluorescence (WDXRF) spectrometer. The Si, Al, Mg and Ce elements calibration curves are made from ICP/DCP standards of 1000 ±4 mg/L for each element. The concentrations are all between 20 and 500 mg/L. All XRF analyses are performed on Myllar films with spectroscopic grade, on which 30 µL of each elemental standard solution is dropped.

The leachates concentrations Ci (kg/m^3) for each i element (Si, Al, Mg or Ce) were deduced from WDXRF spectrometric calibration curves. The i element mass loss, NLi (kg/m^2), for each time range, taken from the test starting time, was calculated using the formula:

$$NLi = Ci \cdot Vo / So \cdot Fi \quad (1)$$

where V: is the leaching mixture total volume (m^3), S is the initial sample surface effectively in contact with the leachate (m^2), and Fi is the i element weight fraction of the GC materials pellet. S (m^2) is assumed to be constant during the tests, and Ci, the initial elemental concentrations in the leachate negligible.

Each i element mean normalized dissolution rate RLi (kg/m^{2}d) was deduced from the mathematical relation number (2). The Origin 8.5 Graph software was used for mathematical calculations.

$$RLi = (Ci^* V)/(fi^* S^* \Delta t) \quad (2)$$

where, Δt: is the test duration in days (d).

Results and Discussion

Materials morphologies and densities

The 7.11 wt.% TiO_2 content glass synthesis was not successful, this glass exhibits a very strong crystallization in the mass during melting. Indeed the substitution of SiO_2 by TiO_2 tightens the glass network despite the fact that the cross-linking the network degree increases, leading consequently to the glass viscosity increase.

This phenomenon was observed by Pierre Mezeix [22] who explained that the addition of 10% TiO_2 increases the viscosity by more than 3 orders of magnitude for a given temperature.

For the other TiO_2 contents in the GC, after the crystallization step, the transparent glassy samples color turns into an opaque dark gray color with brown reflections (Fig. 1). On the cross-sections of the glass-ceramics, one can observe with the naked eye a relatively clear difference in appearance between the surface and the bulk of the samples, which has a darker gray color in the materials bulk compared to the surface color.

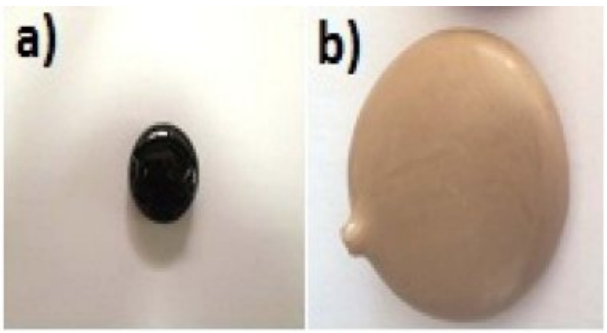

Fig. 1. General appearance of synthetic GC materials, (a) Parent glass after fusion and (b) Parent glass after crystallization.

The obtained GCs density with different TiO_2 contents is determined by the Archimedes method. The results are given in Table 2.

The GC density varies randomly with the TiO_2 content. In general, it is between 2.8913 g/cm^3 and 2.9618 g/cm^3, for GC' TiO_2 contents ranging from 4.11 to 6.11%. Overall, the results are close the other nuclear GC materials densities reported in the literature. GC with diopside (PNC 62) and diopside (PNC 718) mineral phases, synthesized in a TiO_2-rich borosilicate glass melted at T_f = 1185 °C and 1120 °C, have densities of 3.01 and 2.94 g/cm^3, respectively. Other GC materials with sphenes minerals formed in their structure have a density between 2.78 and 2.95 g/cm^3 [23]. A. Quintas et al. [24] synthesized a GC from a Lu-aluminoborosilicate glass, for high-level waste (HLW) sequestration, at a melting temperature of 1350 °C and a crystallization step at Tc = 934 °C. They report a density of 2.946 g/cm^3. This value closest to our experimental values.

T. Wakihara et al. [25] studied the TiO_2 content effect in a glass in the system Y-Si-Al-O-N melted at 1700 °C, and concluded in a random density variation with the TiO_2 content. All the reported values are over 3.5 g/cm^3, and are higher than the GC densities of the present GC materials. Yttrium (Y) of atomic mass 88.90 amu being the preponderant dopant in the studied glass contributed to increase the material density.

Microstructural characterization

The studied GCs diffractograms are gathered in Fig. 2. The phases' identification at different TiO_2 contents is given in Table 3.

Table 2. The GC Archimedes density (ρ_A) as a function of TiO_2 content

GCs	GC1	GC2	GC3	GC4
TiO_2 (%)	4.11	5.11	6.11	7.11
ρ_A (g/cm^3)	2.9618	2.8913	2.9192	–

Table 3. The GCs' phase identification for different contents of TiO_2

GC	TiO_2 (wt.%)	Semi-quantitative composition (%)		JCPDS data [18]
GC1	4.1	77%	$Mg_{0.6}\ Al_{1.2}\ Si_{1.8}\ O_6$	01-075-1568
		11%	$CaMoO_4$	01-085-0585
		10%	$Li_2Fe_5Cr_5O_{16}$	01-073-0213
		1%	$KFeO_2$	01-083-2153
GC2	5.1	77%	$Mg_{0.6}Al_{1.2}Si_{1.8}O_6$	01-075-1568
		9%	$CaMoO_4$	01-085-0585
		11%	$Ca_2\ Zr_5\ Ti_2\ O_{16}$	01-077-1131
		3%	$Pr_{15}\ Ni_7\ Si_{10}$	01-077-1647
GC3	6.1	70%	$Mg_{0.6}Al_{1.2}Si_{1.8}O_6$	01-073-2338
		15%	$CaMoO_4$	01-085-0585
		12%	$Ca_2Zr_5Ti_2O_{16}$	01-077-1131
		3%	$Ba_{0.905}Ca_{0.08}(TiO_3)$	01-082-2234
GC4	7.1	–		–

Except for GC7, for the whole materials, the main formed crystalline phase is the aluminosilicate, of the pyroxene family (Si_2O_6), which is known to be a containment barrier against radionuclide dissipation. Its crystal structure is orthorhombic or monoclinic. Its content in the GC is more than 70%. For 4.11 and 5.11 wt.% TiO_2 GCs, the XRD semi-quantitative analysis gave: 77% of $Mg_{0.6}Al_{1.2}Si_{1.8}O_6$ pyroxene phase (JCPDS N°01-075-1568), 10% of $CaMoO_4$ (JCPDS N° 01-085-0585) and 13% of $Ca_2Zr_5Ti_2O_{16}$ calzirtite phase (JCPDS N° 01-077-1131). The phases presence means that ions in the glass matrix are moving and reacting [26]. The calzirtite formation, is favored by the raising in TiO_2 content in the GC materials. It increases to 25% for the 6.11 wt.% TiO_2 content GC. One can conclude that for the whole TiO_2 contents in the materials, (4.11 to 6.11 wt.%), the GC microstructure contains self-irradiation highly resistant crystals, which are able to confine radioactive waste elements [27].

One can note that calzirtite is identified by HJ Rossell [28] in a similar glass system, $CaO\text{-}ZrO_2\text{-}TiO_2$ system, melted at temperatures below 1370 °C. Yu-Han and Wu Taiwan [29] have also investigated a comparable GC material: a Ti-Zr-rich Li-aluminosilicate, and identify calzirtite minerals. These last authors observed the

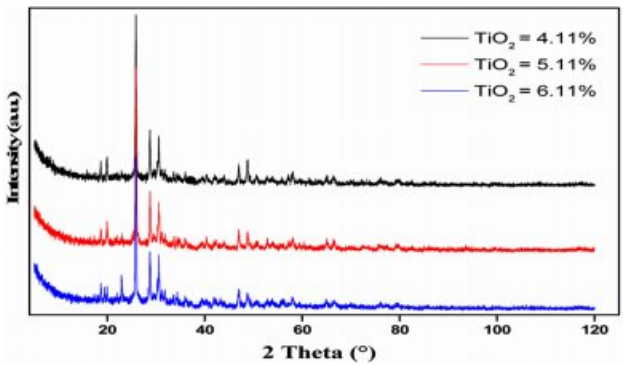

Fig. 2. XRD diffractogramms of glass-ceramics with different contents of TiO_2.

formation of β-quartz phase at low crystallization temperature Tc = 750 °C, which transforms in a pyroxene-type β-spodumene at 880 °C. L.S. Bozadzhiev et al. [30] also observed an isomorph (Ca,Na)(Mg,Fe,Al)(Si, $Al)_2O_6$ pyroxene phase which forms a solid solution with radioactive waste elements as : Sr, Ba, Zr, Y, Ga, Ce, Pr, Nd, Gd, etc. These phases are obtained from a basanite GC containing radionuclides surrogates from I-VIII group (5-15 wt.%). The materials were melted at 1450 °C, and crystallized at 950 °C. M. Chavoutier et al.[31] have synthesized Ti-rich GC materials in the system SiO_2, Li_2CO_3, Al_2O_3, ZrO_2 and TiO_2, with a double-melting at 1450 °C. They observe the spodumene phase (Si_2O_6) germination for a Tc temperature above 1105 °C. From all these results, it appears that a crystallization heat treatment at a temperature greater than 950 °C, in systems comparable to the one we used, promotes the aluminosilicate formation, of the pyroxene family. This is the case for the GCs currently studied, which crystallize at 1010 °C.

The SEM observations were carried out on the samples cross sections. They are depicted on Fig. 3. Such micrographs allowed us to observe both types of phases: crystalline and glassy ones, and confirm the crystalline phases nature identified by XRD analysis. The samples are fully ceramized. The dark prisms are characteristics features of pyroxene phase's germination in most samples. This form often appears in the mono-

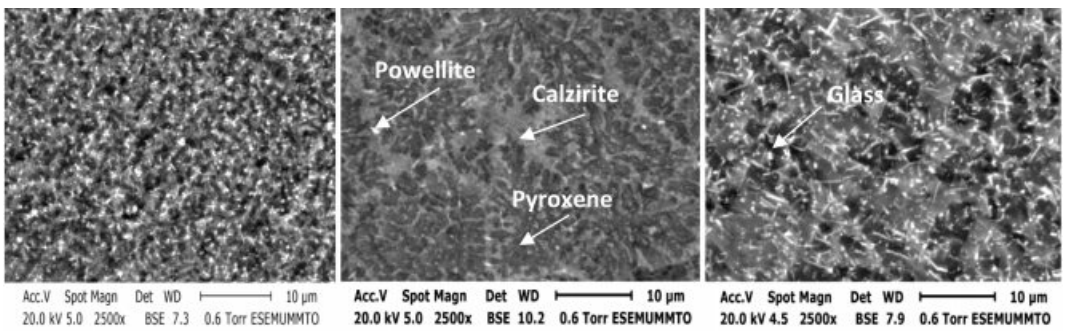

Fig. 3. SEM micrographs of the GC materials with different TiO_2 contents. (a) 4.11 wt.% TiO_2-GC, (b) 5.11 wt.% TiO_2-GC, and (c) 6.11 wt.% TiO_2-GC.

clinic structure. Some authors describe these prisms as "stocky" forms [29, 32]. The calzirite crystals are dipyramidal but light in color. They appear as small piles on the micrographs contrast [27]. The phases appearing in clear platelets are tetragonal powellite crystals [33].

Fig. 4 shows the DTA curve with different TiO_2 contents. For the GC with 5.11 wt.% TiO_2, the parent glass crystallization temperature appears around 563 °C. An allotropic transformation of the calzirtite ($Ca_2Zr_5Ti_2O_{16}$) crystal from monoclinic to tetragonal is revealed around 990 °C for the three GC at different TiO_2 contents. It should be noted that the calzirtite crystal, $Ca_2Zr_5Ti_2O_{16}$, is often associated with that of zirconolite in magma-type rocks, and shows slight variations in their composition, especially the substitution type with respect to lanthanides and actinides, found in trace amounts in these rocks [34]. An allotropic transformation around 1090 °C and 1150 °C, attributable to the pyroxene and wollastonite crystal (pyroxenoids family) respectively, is observed for the three GCs at different TiO_2 contents. M. Chavoutier et al [31] report the spodumene phase transformation, a compound from the same family as pyroxene, around 1050 °C, in a GC made from a Li_2O-Al_2O_3-SiO_2 type glass. Indeed, H. Khedim et al. [10] show a transformation, attributed to the pseudo wollastonite formation at 1170 °C. The ternary phase diagram of: SiO_2-Al_2O_3-CaO illustrates well the range of phases existence. We note that the $CaMoO_4$ allotropic transformations (630 and 690, 810 and 880 °C) are undetectable on the DTA diagrams, because the content of this molybdate is very low and therefore the transformations are not apparent on the spectra. Finally, no melting phenomenon is observed up to 1450 °C.

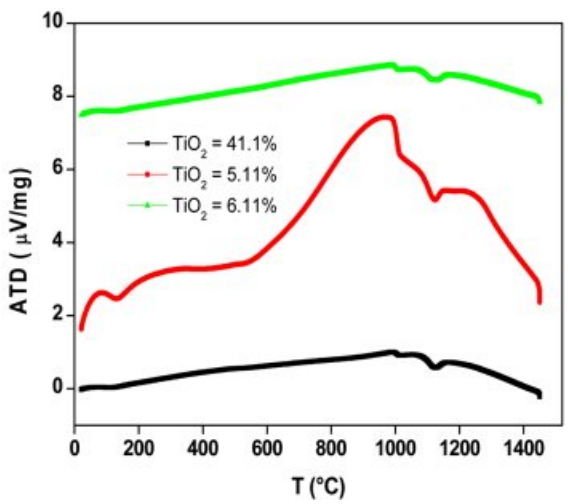

Fig. 4. DTA curve of GC materials with different TiO_2 contents.

Table 4. Allotropic transformation of the different crystalline phases identified in the GCs of different TiO_2 contents

Crystalline phases	Allotropic transformation (°C)			
	GC1	GC2	GC3	GC4
Calzirtite ($Ca_2Zr_5Ti_2O_{16}$)	999.1	986.1	997.4	–
Pyroxene ($Mg_{0.6}Al_{1.2}Si_{1.8}O_6$)	1096.3	1085.2	1083.8	–
Wollastonite ($CaSiO_3$)	1142.1	1142.7	1143.1	–

The Allotropic transformation of the different crystalline phases observed for the GC materials with various TiO_2 contents is given in Table 4.

The FTIR analysis with different TiO_2 contents gave the spectra gathered on Fig. 5. It highlight an absorption band at 1427.1 cm^{-1} corresponding to the Ba-O vibration [35]. In the spectrum region from 1100 to 1200 cm^{-1}, the band corresponding to the presence of [SiO_4] tetrahedra is almost non-existent. Si-O-Si and amorphous SiO_2 bond vibrations at 1083.0, 1081.4, and 1081.7 cm^{-1} for GCs: GC1, GC2, and GC3, respectively. This absorption band is reported at 1080 cm^{-1} in pure glass [36]. The observed shift is due to compositional differences in the synthesized GCs. The characteristic band of the ring structure of [SiO_4] tetrahedra is observed at 775.2, 774.8, 776.7 cm^{-1}, for GCs: GC1, GC2 and GC3, respectively. The latter is quoted at 775 cm^{-1} in the literature. This band is very weak indicating the strong parent glass ceramization. It also indicate the Si-O-Me presence bonds, in Si-Al-Me (Al, Mg) based glass system [35, 37].

The Ti-O elongation vibration appears at 440, 436 and 455 cm^{-1}, for the glass ceramics: GC1, GC2 and GC3, respectively. This band appears at 455.7 cm^{-1} in the literature. The Ti-O elongations bonds characteristic of the formation of the Ti-O-Ti bridge appear in the range 493-456 cm^{-1} [37]. The absorption band around 405 cm^{-1} for GCs: GC1, GC2 and GC3, correspond to the vibration of Zr-O. This band is known to occur at 400 cm^{-1} [39]. It indicates the presence of calzirtite with a $Ca_2Zr_5Ti_2O_{16}$ skeleton in greater proportion in GC3 (12%) than in the other GCs. Overall, we can conclude that these spectra are representative of the studied GCs complex chemical composition.

Chemical durability

The elemental mass loss variation of Si, Al, Mg and

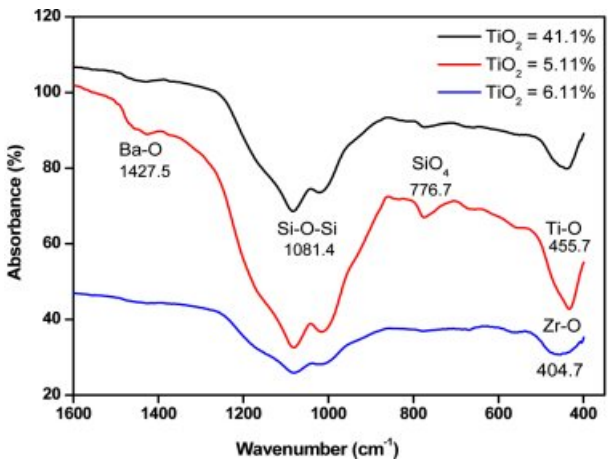

Fig. 5. FTIR spectra of the GCs with different contents of TiO_2.

Ce (actinide surrogate) elements (NL) and the elemental leaching rate of Si, Al, Mg and Ce elements (RLi) are calculated using the formulas (1) and (2) presented in section 1, respectively.

For Si and Mg, the MCC2 test leads to a leaching equilibrium, but for different GCs at values of: 3.4593×10^{-5} kg/m^2 of Si for GC1, 11.9431×10^{-5} kg/m^2 and 14.4076×10^{-5} kg/m^2 of Mg for GC2 and GC3 respectively. For Ce, the whole tests lead to a steady state, except for GC2 leached in MCC1.The GC that leaches the least Ce is GC1 leached in MCC2, with 4.5837 kg/m^2 of Ce. For Al, NL is increasing for all TiO_2 contents in GCs, whatever the employed leaching test. Therefore, Al is not redeposited on the GCs as a passivation layer under the present operating conditions. The best result is for GC2, leached in MCC2. We can conclude that MCC2 test is favorable for leaching unlike the MCC1 test; the high temperature is therefore a limiting factor for the GC elements release, except for Al, for which the concentration doesn't stabilize in the leachates at the end of test. T. Geisler et Al. [40] studied the leaching of a borosilicate glass with a composition similar to that of a German nuclear glass (54.0 SiO_2, 14.8 B_2O_3, 2.4 Al_2O_3, 1.1 TiO_2, 1.8 MgO, 4.8 CaO, 2.9 Li_2O, 7.2 Na_2O, 10.0 CeO_2) in an acidic medium (1M HCl, at 150 °C).This high temperature test, compared to our results for GC1 (4.11 wt.%), leached in MCC2 shows that these values are of the same order of magnitude with our study. They are lower than our values for Al: 8.847×10^{-5} kg/m^2 (12.4783×10^{-5} kg/m^2), and higher than our values for Mg: 9.579×10^{-5} kg/m^2 (8.8626×10^{-5} kg/m^2) and Ce 9.10×10^{-5} kg/m^2 (4.5837×10^{-5} kg/m^2) and Si: 0.44×10^{-5} kg/m^2 (26.0148×10^{-5} kg/m^2).

The leaching rate (RL) of Si, Al, Mg and Ce as a function of time, for each material doped with different TiO_2 contents are gathered on Fig. 6, for all the tests (MCC1 and MCC2). For Si, leaching equilibrium is achieved for all GCs and for both leaching tests. The leaching rate in Si is also negligible. The best leaching rate is 61.47×10^{-9} kg/m^{2}d in Si for GC1 leached in MCC2. This represents a GC1 mass percentage present in the leachate of 0.015%. All the GCs show a stabilization of the Mg leaching rate, at the end of MCC2 test. The best Mg leaching rate is 191.94×10^{-9} kg/m^{2}d for GC2 leached in MCC2, which represents a GC1 Mg mass percentage present in the leachate of 0.047%. This rate is negligible after 14 leaching days. The sole GC that shows a decrease in Al leaching rate is GC1 leached in MCC2 test, which reaches 48.9 10^{-9} kg/m^{2}d, representing a mass content present in the leachate relative to the total amount in GC1 of 0.25%. These results are predicted by the presence of sphene:

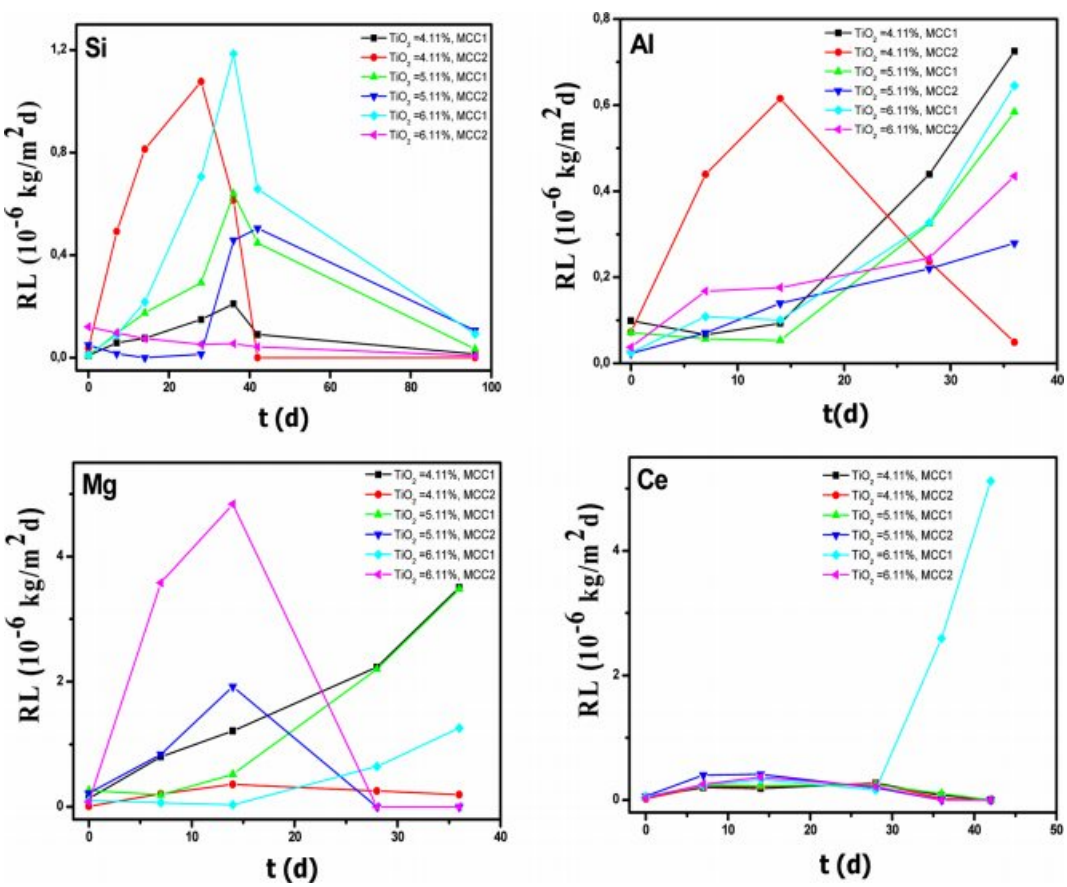

Fig. 6. Elemental leaching rates (RL_i) of Si, Al, Mg and Ce as a function of time for the GCs with different TiO_2 contents, leached in both MCC1 and MCC2 tests.

$Mg_{0.6}Al_{1.2}Si_{1.8}O_6$ with a content of 77% in both GC1 and GC2), which constitutes a double barrier. S. Gavarini [41] reports much higher Si leaching rate values (23×10^{-3} kg/m^{2}d and 50×10^{-3} kg/m^{2}d) for the leaching of Ce-rich glasses with chemical formula CeYSiAlO when leached in static mode at 90 ºC in a closed system. For Ce, the steady state is reached for all GCs in both leaching tests, except for GC3 leached in MCC1 test. The leaching rate in Ce is also negligible. The best leaching rate is 193.7×10^{-9} kg/m^{2}d in Ce for GC2 leached in MCC2; this represents a GC2 Ce mass percentage released in the leachate of 0.032%. This value complies with nuclear industry requirements ($<10^{-3}$ kg/ m^{2}d) [42,43]. The best results are for GC with 4.11 and 5.11% TiO_2 for the MCC2 test.

Conclusion

In this study, we performed the synthesis and characterization of glass-ceramic matrices, based on an aluminosilicate glass, in the system SiO_2-Al_2O_3-CaO-MgO-ZrO_2-TiO_2, with four different TiO_2 contents ranging from 4.11 to 7.11 wt%. These GC confinement matrices are intended to confine in their structure both fission products and lanthanides elements, from radioactive waste. The GC synthesis is done in several steps: a double fusion of the oxides mixture at 1350 ºC, a nucleation at 564 ºC, and a crystal growth at 1010 ºC. The GC synthesis for the material with 7.11 wt.% TiO_2 content, was not successful. For the others materials, the obtained GC have Archimedes densities in the range from 2.891 to 2.962 g/cm^3. Except for the GC with 7.11 wt.% TiO_2, the XRD phase identification show that the main formed phases in the materials are pyroxene, powelite and calzirtite phases, which are known as self-irradiation resistant phases. The SEM confirmed the morphological aspect for these phases in the microstructures. The DTA analysis reveals the allotropic transformations for these phases. The FTIR analysis spectra are representative of the studied glass-ceramics complex chemical composition. MCC1 and MCC2 tests, performed on selected glass ceramic materials among the different TiO_2 contents GCs, indicate that the materials with 4.11 wt.% and 5.11 wt.% TiO_2 have the best leaching behavior, for MCC2 test (90°C), for the four analyzed elements (Si, Al, Mg and Ce).The leaching rate in Ce (actinide surrogate) is negligible. The best leaching rate is 193.7×10^{-9} kg/m^{2}d after 28 leaching days in Ce for 5.11 wt.% leached in MCC2. The studied GCs with different TiO_2 contents matrix are strongly recommended for the disposal of high-level waste.

References

1. J. Hiet, Motifs structuraux dans des verres modèles pour le stockage des actinides, Université d'Orléans (2009) 01-09.
2. P.J. Hayward, Glass Technology,29 (1988) 122-136.
3. W. Lutze, R.C. Ewing, in "Glass-ceramics in radioactive waste forms for the future" (Elsevier Science Pub B. V Amsterdam, 1988) p.427-494.
4. I. Donald, B. Metcalfe, R.J. Taylor, J. Mater. Sci 32 (1997) 5851-5887.
5. W. Lee, M. Ojovan, M. Stennett, and N. Hyatt, Adv. Appl. Ceram, 105 (2006) 3-12.
6. R. Souag, N. Kamel, M. Hammadi, Z. Kamel, D. Moudir, F. Aouchiche, Y. Mouheb and S. Kamariz, J. Ceram. Process. Res. 16[1] (2015) 150-155.
7. M.-S. Paizullakhanov, I. Atabaev, S. Faiziev, Int. J. Mining. Sci. 2(2016) 8-12.
8. W. Holand, G. Beall, in "Principles of designing glass-ceramic formation, Glass-ceramic technology"(Westerville, 2002) p.1-73.
9. E. Maddrell, S. Thornber, N.C. Hyatt, J. Nucl.Mater 456 (2015) 461-466.
10. H. Khedim, H. Nonnet, F.O. Méar, J.Power Sources, 216 (2012) 227-236.
11. P. Loiseau, D. Caurant, O. Majerus, N. Baffier, C. Fillet, MRS Online Proc. Libr, 807 (2003) 333-338.
12. M.V. Alencar, G.V. Bezerra, L.D. Silva, J.F. Schneider, M.J. Pascual, A.A. Cabral, J.Non-Cryst. Solids, 554 (2021) 120605.
13. S. Salama, E.A. Saad, H. Darwish, H. Abo-Mosallam, Ceram. Int, 31 (2005) 559-566.
14. M. Lu, F. Wang, Q. Liao, K. Chen, J. Qin, S. Pan, J. Mol. Struct, 1081 (2015) 187-192.
15. X. Liu, J. Zhou, S. Zhou, Y. Yue, J. Qiu, Prog. Mater. Sci, 97 (2018) 38-96.
16. F. Wang, M. Lu, Q. Liao, Y. Wang, H. Zhu, G. Xiang, L. Li, Y. Zhu, Mater.Chem. and Phys, 239 (2020) 122314.
17. Nour-el-Hayet Kamel, D.Moudir, Z. Kamel, A. Djeridi, S. Mouhamou, A. Benmounah, R. Souag, M. Taouinet, H. Ait-Amar, J.Mater.Sci and Eng A, 3 (2013) 209-223.
18. R. Souag, N. Kamel, Y. Mouheb, M. Hammadi, Z. Kamel, D. Moudir, F. Aouchich, S. Kamariz, Sci.Sinter, 46 (2014) 377-383.
19. P. JCPDS, Diffraction Data CD-ROM, International Center for Diffraction Data, Newtown Square, PA, (2004).
20. Omnic, Nicolet instrument, 1992-2001.
21. M.I. Ojovan, W.E. Lee, Metall. Mater. Trans A, 42 (2011) 837-851.
22. P. Mezeix, in "Verres et vitroceramiques du systeme BaO – TiOff – SiOff : elaboration, proprietes mecaniques et couplage mecanoelectrique. Optique [physics.optics]" (Universite Rennes 1, 2017) p.46-47.
23. I.W. Donald, in "Waste immobilization in glass and ceramic based hosts: radioactive, toxic and hazardous wastes" (John Wiley & Sons, 2010) p.333-334.
24. D.C. A. Quintas, O. Majérus, Proc. XXI Int. Congr. Glass-Strasbourg, France, 1-7 July (2007).
25. T. Wakihara, J. Tatami, K. Komeya, T. Meguro, A. Kidari, S. Hampshire, M.J. Pomeroy, J. Eur. Ceram.Society, 32 (2012) 1157-1161.
26. F. Wang, L. Guo, C. Wang, F. Ye, J. Eur. Ceram. Society, 37 (2017) 289-296.
27. I. Bardez, P. Loiseau, D. Caurant, N. Baffier, and C. Fillet, Etude de céramiques et de vitrocéramiques à base de zirconolite-Hf (CaHfTi2O7) destinées au confinement de déchets nucléaires de haute activité, Tours, France. ffhal-00177934 (2002).
28. H. Rossell, J.of Solid State Chem, 99 (1992) 52-57.
29. Y.-H. Wu, K.-C. Hsu, C.-H. Lee, Ceram. Int, 38 (2012)

4111-4121.
30. L. Bozadzhiev, G. Georgiev, R. Bozadzhiev, Sci. Sinter, 43 (2011) 225-229.
31. M. Chavoutier, D. Caurant, O. Majérus, R. Boulesteix, P. Loiseau, C. Jousseaume, E. Brunet, E. Lecomte, J.Non-cryst. solids, 384 (2014) 15-24.
32. P. Alizadeh, V. Marghussian, J.Eur.Ceram. Society, 20 (2000) 775-782.
33. D. Caurant, O. Majerus, E. Fadel, M. Lenoir, C. Gervais, O. Pinet, J. Am. Ceram.Soc, 90 (2007) 774-783.
34. M.-L. Pascal, A. Di Muro, M. Fonteilles, C. Principe, Mineral.Mag, 73 (2009) 333-356.
35. M. Sales, J. Alarcon, J. Mater. Sci, 30 (1995) 2341-2347.
36. N. Nagai, H. Hashimoto, Appl. Surf. Sci, 172 (2001) 307-311.
37. R. Petrović, D. Janaćković, S. Zec, S. Drmanić, L. Kostić-Gvozdenović, J. Sol-gel Sci.Technol, 28 (2003) 111-118.
38. T. Bezrodna, G. Puchkovska, V. Shymanovska, J. Baran, H. Ratajczak, J.Mol. Struct, 700 (2004) 175-181.
39. I.H. Joe, A.K. Vasudevan, G. Aruldhas, A. Damodaran, K. Warrier, J.Solid State Chem, 131 (1997) 181-184.
40. T. Geisler, A. Janssen, D. Scheiter, T. Stephan, J. Berndt, A. Putnis, J.Non-Cryst. Solids, 356 (2010) 1458-1465.
41. S. Gavarini, in "Durabilite chimique et comportement a l'irradiation des verres quaternaires LnYSiAlO (Ln= La ou Ce)" (Universite d'Orleans, 2002) p.144-146.
42. L. Wu, H. Li, X. Wang, J. Xiao, Y. Teng, Y. Li, J. Am. Ceram. Soc, 99 (2016) 4093-4099.
43. Chian Standards, No. EJ 1186-2005 (2005) p.4-11.